

Published in final edited form as:

*Proteomics Clin Appl.* 2010 January ; 4(1): 4–16. doi:10.1002/prca.200900050.

## Proteomic examination of *Leishmania chagasi* plasma membrane proteins: contrast between avirulent and virulent (metacyclic) parasite forms

Chaoqun Yao<sup>1,7,8,\*</sup>, Yalan Li<sup>5</sup>, John E. Donelson<sup>2,6</sup>, and Mary E. Wilson<sup>1,3,4,6,7</sup>

<sup>1</sup>Department of Internal Medicine, University of Iowa, Iowa City, IA 52242

<sup>2</sup>Department of Biochemistry, University of Iowa, Iowa City, IA 52242

<sup>3</sup>Department of Microbiology, University of Iowa, Iowa City, IA 52242

<sup>4</sup>Department of Epidemiology, University of Iowa, Iowa City, IA 52242

<sup>5</sup>Department of Proteomics Facility, University of Iowa, Iowa City, IA 52242

<sup>6</sup>Department of Program in Cellular and Molecular Biology, University of Iowa, Iowa City, IA 52242

<sup>7</sup>VA Medical Center, Iowa City, IA 52246

<sup>8</sup>Department of Veterinary Sciences and Wyoming State Veterinary Laboratory, University of Wyoming, Laramie, WY 82070

### Abstract

Leishmaniasis annually leads to two million new cases with 59 thousand deaths worldwide. Promastigotes of the causative *Leishmania* spp. develop from procyclic (log) to the highly virulent metacyclic stage within the sand fly vector. We hypothesized that proteins important for promastigote virulence might be uniquely represented in the plasma membrane of metacyclic, but not log, promastigotes. Purified metacyclic promastigotes from stationary phase cultures of *Leishmania chagasi* were applied to prepare membrane preparations either by surface biotinylation-streptavidin affinity separation or by octyl glucoside detergent extraction. These membrane fractions were enriched over 130 and 250 fold, respectively, estimated by western blotting for the plasma membrane marker MSP. A total of 447 or 33 proteins were identified by surface biotinylation or detergent extraction, respectively, by LC-MS/MS. Confocal microscopy suggested the difference between the lists was due to the fact that proteins localized both on the surface membrane and within the flagellar pocket were accessible to surface biotinylation. Using detergent extraction, we found different proteins were present in membrane proteins of logarithmic stage compared to metacyclic stage promastigotes. Several dozens were stage specific. These data provide a foundation for identifying virulence factors in the plasma membranes of *Leishmania* spp. promastigotes during metacyclogenesis.

### Keywords

*Leishmania*; metacyclic promastigotes; plasma membrane proteins; proteomics

**To whom all correspondence should be sent:** Dr. Chaoqun Yao, Department of Veterinary Sciences and Wyoming State Veterinary Laboratory, University of Wyoming, Laramie, WY 82070; Tel (307)742-6638; Fax (307)721-2051; cyao@uwyo.edu.

### Conflict of interest statement

All authors have no conflict of interest.

## Introduction

The digenetic *Leishmania* spp. protozoa shuttle between a sand fly vector, where they exist as flagellated promastigotes, and a mammalian host, in which they survive as non-flagellated amastigotes. Aflagellate intracellular amastigotes ingested by the sand fly during its blood meal transform to flagellated procyclic promastigotes in the midgut of the sand fly. Procyclic promastigotes transform through the nectomonad, leptomonad and haptomonad stages and eventually develop to metacyclic promastigotes, in a developmental process that is called metacyclogenesis [1]. Some aspects of metacyclogenesis can be approximated *in vitro* during growth of promastigotes in liquid cell culture [2,3]. Methods to purify culture-derived metacyclic-like promastigotes have been developed for *Leishmania major* [4], *L. donovani* [5] and *L. chagasi* [6]. Metacyclic promastigotes appear in large numbers behind the stomodeal valve of the sand fly and migrate freely, resulting in some organisms moving anteriorly to the foregut and mouth parts. From here the promastigotes are inoculated into a pool of blood in the skin of humans and other mammals when the fly takes another blood meal. Metacyclic promastigotes are then phagocytosed by host macrophages and transform into aflagellate amastigotes [7,8].

During metacyclogenesis, promastigote virulence for experimental mammalian models increases significantly. The expression of a number of surface-exposed virulence factors is increased during metacyclogenesis, including lipophosphoglycan [9–11], major surface protease (MSP, also called GP63), and GP46 (also called promastigote surface antigen protein 2) [12,13]. The goal of the current study was to use the tools of proteomics to contrast between avirulent and virulent promastigotes and thereby identify as yet unrecognized potential virulence factors amongst the plasma membrane proteins of *Leishmania* spp. metacyclic promastigotes. We identified dramatically different numbers of proteins with different protocols to prepare membrane-associated proteins, differences that were attributable to whether or not proteins from the flagellar pocket were included in the preparation. Using the more stringent method, which identified only surface and microsomal membrane proteins, we found that several dozen proteins were specific to promastigotes in either their logarithmic or their metacyclic stages of growth. This study provides a solid foundation for further investigation of virulence factors in these trypanosomatid protozoa.

## Materials and Methods

### Parasites

The Brazilian strain MHOM/BR/00/1669 of *L. chagasi*, originating from a patient with visceral leishmaniasis [14], was continuously passaged by intracardiac injection of amastigotes in golden hamsters to maintain virulence. Amastigotes were isolated from the spleens of infected hamsters and transformed to promastigotes at 26°C in hemoflagellate-modified minimal essential medium (HOMEM; reagents from GIBCO, Rockville, MO) with 10% heat-inactivated fetal calf serum. Promastigote cultures were started at a density of  $1 \times 10^6$  cell/ml at day 0 of cultivation using virulent promastigotes within five passages. Metacyclic promastigotes were isolated to homogeneity from day 8 stationary cultures by a discontinuous Ficoll gradient as previously described [4,6].

### Plasma-membrane protein isolation

Two protocols to isolate promastigote surface membrane proteins were compared. (1) Surface biotinylation. Metacyclic promastigotes were surface biotinylated by incubation at room temperature (RT) for 1 h in 1 mM Sulfo-NHS-SS-Biotin (Pierce, Rockford, IL) in Hanks' balanced salt solution (HBSS, GIBCO) as described [15,16]. Subsequent steps were

all performed at 4°C. The surface biotinylated metacyclic promastigotes were lysed by agitation in 2% NP-40/HBSS for 16 h. More than 95% lysis was consistently achieved, according to microscopic monitoring. The lysates were subjected to two sequential centrifugation steps at 3,000 and 10,000 ×g (10 min each). The resultant supernatants were agitated with streptavidin agarose beads (Sigma, St. Louis, MO) for a minimum of 1 h. The biotinylated proteins were collected and washed twice in 0.5% Triton X-100 in TBS (10 mM Tris/HCl, 140 mM NaCl, pH 7.4) and twice in TBS by centrifugation at 10,000 ×g for 1 min. Proteins were released from the agarose beads by heating at 100°C for 5 min in SDS-PAGE sample buffer with β-mercaptoethanol (βME) as a reducing reagent to break disulfide bonds bridging the labeled proteins and biotin [15,16]. For 2DE, the beads were incubated in an IEF lysis buffer containing 7 M urea, 2 M thiourea, 5% βME and 6% ampholytes with non-ionic detergent 2% NP-40, 4% CHAPS or 1% ASB-14 [17].

(2) Freeze thaw in hypotonic buffer. As an alternative approach to collecting membrane-enriched fractions, metacyclic or procyclic promastigotes were lysed by incubation in a hypotonic buffer (1 mM K acetate, 1.5 mM Mg acetate, 1 mM CaCl<sub>2</sub>, 10 mM Tris, 2 mM EDTA, pH 7.2) on ice with DNase/RNase and protease inhibitor cocktails (Calbiochem, Gibbstown, NJ) at 4°C for 30 min, followed by five cycles of freezing in -80°C and thawing in a RT water bath. Cell lysis was microscopically monitored, and more than 90% cell lysis was consistently achieved. After removal of non-lysed cells from total cell lysates by 1,000 ×g centrifugation (6 min, 4°C), samples were subjected to 100,000 ×g centrifugation (1 h, 4°C) and the pellets containing both microsomes and membranes were collected. Pellets were resuspended in 2% octyl glucoside (Sigma) in 10 mM Tris, pH 7.5 with DNase/RNase followed by incubation on ice for 20 min. Membrane proteins were recovered from the supernatants of 178,000 ×g centrifugation (20 min, 4°C) [18,19], and boiled in SDS-PAGE sample buffer with βME and subjected to SDS-PAGE. Some preparations of membrane proteins were precipitated with 10% TCA, and directly subjected to LC-MS/MS analysis.

### Electrophoresis and western blots

Proteins for IEF were solubilized in 300 μl of IEF lysis buffer and applied directly to rehydrated 11 cm gel strips of Immobiline™ DryStrip pH 3–10 (GE Healthcare, Piscataway, NJ) for 16 h at RT. The strips were subjected to 50,000 V-hours for IEF at 20°C. SDS-PAGE was carried out on 5–15% polyacrylamide gels. Proteins in SDS-PAGE gels were either directly visualized by silver staining following the manufacturer's protocol (SilverQuest Silver Staining Kit, Invitrogen, Carlsbad, CA), or were blotted onto nitrocellulose filters (Schleicher & Schuell BioSciences, Keene, NH) followed by western blotting. Filters were alternately incubated with sheep polyclonal antiserum (1:10,000 dilution) directed against purified *L. chagasi* MSP [19], goat polyclonal antiserum (1:5,000 dilution) against recombinant P36, a cytosolic protein of *Leishmania* spp. [6,20], rabbit polyclonal antibody to ER luminal protein BiP (1:1,000 dilution, kindly provided by Dr. J. Bangs of the University of Wisconsin), and a monoclonal antibody against α-tubulin (AB-1, 0.1 μg/ml, Oncogene, San Diego, CA). Peroxidase conjugated anti-sheep and anti-goat antisera were purchased from Kirkegaard & Perry Laboratories (Gaithersburg, MA), whereas anti-rabbit and anti-mouse antisera were from CalBioChem, and Bio-Rad Laboratories (Richmond, CA), respectively. All secondary antibodies were used at a 1:10,000 dilution.

### LC-MS/MS

Gel slices from silver-stained SDS-PAGE gels were incubated in destain solution (Invitrogen SilverQuest Silver Staining Kit), followed by rehydration in water. The gel slices were washed once each in 25 mM NH<sub>4</sub>HCO<sub>3</sub> and 50% ACN dissolved in 25 mM

NH<sub>4</sub>HCO<sub>3</sub>. Dried gels were sequentially treated in 10 mM DTT for one hour at 56°C, and 55 mM iodoacetamide at RT in the dark with occasional agitation for 45 min for reduction and alkylation, respectively. After another round of rehydration and dehydration followed by complete drying, gels were rehydrated in appropriate volumes of 8 ng/μl sequencing-grade trypsin solution (Promega, Madison, WI) on ice for 10 min, followed by incubation at 37°C for 16 h.

Tryptic peptides were extracted from gels by sonication and incubation in 50% ACN with 0.1% formic acid. This was repeated once and the supernatants were combined. The supernatant volumes were reduced by Speedvac. The samples along with the washes in a total volume of 15 μl were then transferred to 200 μl inserts and 3 μl of each sample were injected into a Thermo Scientific LTQ XL linear ion trap mass spectrometer equipped with ETD and Eksigent NanoLC-1D using a C18 column (75 μm × 10 cm, New Objective, Woburn, MA). Flow rates were set at 200 nl/min with standard gradients composed of mixtures of ACN and water with 0.1% formic acid. A data-dependent MS survey scan between 400 and 2000 was performed followed by 10 MS/MS scans to detect the 10 most abundant ions with CID. Mass dynamic exclusion was applied.

For protein identification, LC-MS/MS data were searched against a database using the SEQUEST algorithm of BioWorks 3.3.1 software (Thermo Fisher scientific Inc., San Jose, CA). The database was created using a local computer on August 2007 by downloading 24,750 entries deposited in GenBank and the published genomes containing the key words *Leishmania*, *Trypanosoma* or trypanosomatid. The published genomes of trypanosomatids include *L. major*, *L. infantum*, *L. braziliensis*, *Trypanosoma brucei* and *T. cruzi* [21–24]. The search parameters were: enzyme specificity considered, trypsin (KR), fully enzymatic cleavage at both ends; number of missed cleavages permitted, 1; fixed modifications including residue specificity, 1 PTM per peptide at cysteine for carboxyamidomethylation; no variable modifications; mass tolerance for precursor ions, 1 AMU; mass tolerance for fragment ion, 1 AMU. The final filter parameters were: 0.100 for Delta CN; and 1.90 (+1), 2.70 (+2), and 3.5 (+3) for Xcorr charge state of each peptide. For each positively identified protein, a minimum of two individual peptides had to satisfy these criteria with a protein score cutoff at e<sup>-6</sup>. Each protein was checked for a transmembrane domain (TMD) and a glycosylphosphatidylinositol (GPI) anchor using TMPred-Prediction of Transmembrane Regions and Orientation ([http://www.ch.embnet.org/software/TMPRED\\_form.html](http://www.ch.embnet.org/software/TMPRED_form.html)), and big-PI Predictor GPI Modification Site Prediction ([http://mendel.imp.ac.at/gpi/gpi\\_server.html](http://mendel.imp.ac.at/gpi/gpi_server.html)), respectively. The defaulted parameters were used during the search processes.

### Confocal microscopy

Surface-biotinylated metacyclic promastigotes, or non-biotinylated control promastigotes, were fixed in 10% PBS-buffered formalin for 16 h. Permeabilized cells were incubated in 0.2% Triton X-100/PBS, whereas non-permeabilized cells were incubated in PBS alone. After blocking in 10% goat serum/PBS, cells were incubated in 1:200 diluted FITC-conjugated extravidin (Sigma) in blocking solution. The cells were suspended in VECTASHIELD® mounting medium (Vector Laboratories, Burlingame, CA) and examined using a Zeiss 510 confocal microscope (Thornwood, NY). Z-series images were recorded for 0.3 μm thick slices.

## Results

### Plasma membrane proteins of metacyclic promastigotes isolated by surface biotinylation-streptavidin affinity purification

Metacyclic promastigotes were isolated from stationary phase promastigotes according to density, using our published modification of a method developed for *L. major*. The method yields a > 95% pure metacyclic population of the cells [4,6]. Surface biotinylation-streptavidin affinity purification yielded a preparation of the exposed proteins available for surface biotinylation in live metacyclic *L. chagasi* promastigotes (Figure 1A). The GPI-anchored MSP proteins were used as markers for plasma membrane proteins on western blots, whereas cytoskeletal  $\alpha$ -tubulin, cytosolic P36 and the ER luminal protein BiP were used to assess the degree of contamination with non-plasma membrane proteins. As clearly shown in Figure 1A, the abundant MSP proteins were presented in the bead pulldown fraction (lane 4), whereas markers for contaminating cytoskeletal ( $\alpha$ -tubulin), cytosol (P36) and organelles (BiP in the endoplasmic reticulum) were below the detectable levels in this lane. In a densitometric analysis no MSP enrichment was found in the lanes 2 and 5. Enrichment indexes calculated from a ratio of cell fractions to the total cell lysates were 0.8, 1.4 and 0.9, respectively, when  $\alpha$ -tubulin, P36 and BiP were used as denominators. In contrast, enrichment indexes for lane 4 were 200.4, 208.9 and 251.4, respectively. Furthermore, an average of 134.3 fold enrichment was observed using  $\alpha$ -tubulin as the denominator (SD=66.4, n=6). These data suggest that plasma-membrane proteins were substantially separated from cytosol, cytoskeleton and internal organelles in the parasite cell by biotin-avidin affinity purification.

Surface biotinylated parasite proteins were separated on 5–15% gradient SDS-PAGE gels and detected by silver staining. No discrete bands could be visualized, an observation that is not unusual for amphipathic membrane proteins. A representative gel was sliced into 40 segments covering the entire lane from top to bottom. After in-gel trypsin digestion and elution followed by LC-MS/MS, up to several dozen proteins were detected in each gel slice. There was good correlation between protein sizes and electrophoretic mobility (Figure 1B). Surprisingly, a total of 447 proteins were detected throughout the 40 gel slices (supplemental Table 1). Similar protein preparations were also subjected to 2DE, which separates proteins sequentially by *pI* and molecular size. Three different non-ionic detergents, NP-40, CHAPS, and ASB-14, were individually used in the first dimension to enhance protein solubility during IEF. Hundreds of proteins were revealed by silver staining. The resolution capacity of the detergents, listed from the best to worst, was NP-40, CHAPS, and ASB-14 (data not shown).

Peptide coverage of the 447 proteins identified by LC-MS/MS was as follows. One-sixth were identified by peptides covering less than 5% of the amino acid residues of the corresponding proteins, one third had 5–10% coverage, and the remainder had more than 10% of the protein covered by peptides, amongst which a few had more than 40% coverage (Figure 2A). In the trypanosomatid protozoa including *Leishmania* spp., many plasma membrane proteins are attached to the parasite surface via a GPI anchor. Others are attached via a TMD or through binding to other membrane-associated molecules. Thus, we further analyzed these 447 proteins for a GPI anchor and a TMD using bioinformatics (see Materials and Methods). Five proteins were found to have a signal for GPI anchor addition, all of which were different MSP proteins. This is consistent with published experimental data indicating that most MSPs possess GPI anchors [13]. More than two-thirds of the 447 proteins were predicted to have at least one TMD with 22 proteins having more than 5 TMDs (Figure 2B and supplemental Table 1). The remaining one-third were not predicted to have a TMD. Although the lack of a predicted TMD does not eliminate a protein from being a plasma membrane protein, these data led us to suspect that the method identified more

proteins than those merely associated with the plasma membrane. We chose a microscopic approach to investigate this possibility, described below.

### **Proteins in the flagellar pockets were readily surface biotinylated**

To examine why so many proteins were included in surface biotinylated fractions we queried which proteins in live promastigotes were accessible to surface biotinylation. We approached this question using confocal microscopy. Surface biotinylated metacyclic promastigotes showed identical staining patterns whether permeabilized or not (Figure 3). As expected, the surface of the cell body and flagellum stained with FITC-avidin with no appreciable intracellular staining. However, staining was stronger in the flagellar pocket than at the cell surface. In contrast, there was no FITC staining of non-biotinylated controls. The flagellar pocket is a unique organelle found in all Trypanosomatid protozoa, that is formed by the invagination of the plasma membrane at the base of flagellum. The flagellar pocket is the sole site of endocytosis and exocytosis in these protozoa. The confocal images show that proteins in the flagellar pocket of trypanosomatids were readily accessible to the membrane-impermeable biotinylation reagents. This provides an explanation for why so many proteins were isolated by surface biotinylation. We surmise that many of the proteins listed in Supplemental Table 1 likely represent proteins in the flagellar pocket trafficking through endocytic/exocytic pathways.

### **Membrane proteins isolated by octyl glucoside extraction**

Because the above data indicate that proteins identified through surface biotinylation and LC-MS/MS included protein contents of the flagellar pocket, an alternative approach to isolate membrane proteins was employed. Membranes were isolated by high speed centrifugation from the whole cellular lysates of metacyclic promastigotes. Afterwards, membrane-associated proteins were extracted with the detergent octyl glucoside, which has the advantage that its low critical micelle concentration allows its removal from membrane protein preparations by dialysis [14,18,19]. Both P36 and BiP were found in the non-membranous fractions (Figure 4A, lane 3). MSP proteins were mostly found in the membrane fraction (lanes 4–5). After extraction with octyl glucoside, membrane fractions contained no detectable contaminants from cytosolic (P36) or ER (BiP) proteins (Figure 4A, lane 5). By densitometric analysis, an enrichment index for this lane was 253.0 (SD=3.7, n=4) and 286.3 (SD=17.3) when P36 and BiP were used as the denominator, respectively. These data demonstrated that highly enriched preparations of membrane proteins were achieved. Membrane proteins were also visualized by silver staining. A smear appeared at the top of the gel covering the protein sizes of 70–150 kDa and three additional bands were observed at 63, 40 and 22 kDa (Figure 4B). In 40 gel slices spanning the entire lane and subjected to LC-MS/MS analysis following trypsin digestion, 33 proteins were identified (supplemental Table 2), of which sixteen were also isolated by surface biotinylation (Table 1, Figure 5). Among these were 5 MSPs, four of which are predicted to have a GPI anchor.

### **Differential expression of plasma membrane proteins during metacyclogenesis**

Metacyclogenesis refers to the process through which noninfectious procyclic promastigotes develop into the infectious metacyclic promastigotes in the sand fly vector [2,3]. We hypothesized that plasma membrane proteins expressed uniquely by metacyclic promastigotes represent potentially important virulence factors. Membrane proteins were isolated by octyl glucoside extraction of either metacyclic or logarithmic growth phase promastigotes; the latter contain a low content of virulent metacyclic parasites. These proteins were subjected to either denaturing and reducing by heating to 100°C in SDS-PAGE sample buffer prior to trypsin digestion, or directly subjected to trypsin digestion followed by LC-MS/MS. Both types of samples yielded similar proteomic results in multiple preparations. Even though the membrane preparations were achieved by the same approach

of octyl glucoside extraction, 33 proteins were identified in gel slices from protein preparations that were separated by SDS-PAGE and excised. In contrast, 60 proteins were identified from the samples that were directly subjected to LC-MS/MS with no prior separation step. With the first approach, it is possible that some proteins were lost between gel slices, and/or that some proteins were left in the gel matrix. As showed in Table 2, 60 and 82 proteins were identified in the membrane of the metacyclic and logarithmic growth phase promastigotes, respectively. Among these, 36 and 58 were stage specific, and only 24 proteins were expressed in both stages.

## Discussion

The plasma membrane of protozoan parasites is a unique cell structure that plays vital roles in maintaining cellular integrity and in facilitating parasite interactions with its different environments. The goal of this study was to characterize plasma membrane proteins uniquely expressed in virulent metacyclic *L. chagasi* promastigotes. We hypothesize that these proteins might play important roles in parasite virulence.

Recent advances in technology have led to the capacity to both quantitative and qualitative proteomics in samples ranging from organs, tissues and cells to subcellular organelles [25–30]. We used the same approach to identify plasma membrane proteins of *Leishmania* promastigotes. Two approaches were attempted to isolate plasma membrane molecules. First, we used avidin affinity purification of proteins that were biotinylated on the surface of intact live promastigotes, a method that has been successfully used to isolate plasma membrane proteins from many different cell types [31–36]. Western blotting demonstrated more than 130 fold enrichment in MSP proteins, markers for plasma-membrane proteins in these biotinylated membrane preparations (Figure 1).

Second, membrane-enriched cellular fractions were separated by centrifugation and membrane proteins were extracted with the detergent octyl glucoside. MSP proteins were enriched over 250 fold, making this method superior to the biotinylation-streptavidin affinity purification approach (Figure 4). Furthermore, a very large number of proteins (447) were identified by biotinylation of live non-permeabilized metacyclic promastigotes, whereas only 33 were present in detergent extracted samples. Microscopic investigation led to the discovery that the contents of the flagellar pocket were strongly labeled by “surface” biotinylation. We conclude that the detergent extraction method yielded a more accurate view of parasite surface exposed molecules. Therefore, membrane proteins were isolated from, and contrasted between, avirulent logarithmic growth phase and virulent metacyclic promastigotes by octyl glucoside extraction. LC-MS/MS identified 58 and 36 stage-specific membrane proteins, respectively.

Sixteen proteins were identified by both live cell biotinylation and detergent extraction (Table 1). This list included five MSPs, of which four have a GPI membrane anchor [12,13], and two vacuolar ATP synthases. The latter are transporters localized in the plasma membrane [37]. Enolase was commonly identified by both approaches. Several groups have published data showing that this protein is localized to the plasma membranes of several types of cells including *L. mexicana* promastigotes, using diverse approaches including biochemistry, genetics, proteomics, cellular fraction, and confocal and immunoelectron microscopy [38–42]. Unexpectedly, both cytoskeletal  $\alpha$ - and  $\beta$ -tubulin were also commonly found, even though they were below the detectable levels by western blotting. The list also contained the cytoskeleton-associated protein CAP5.5. One plausible explanation is that some cytoskeletal proteins are tightly associated with plasma membrane proteins, and therefore are co-isolated with the latter. This could reflect the extensive subpellicular microtubules in *Leishmania* closely apposed to the inner surface of the plasma membrane,

possible through a link corresponding to the cytoplasmic portion of integral membrane proteins such as P60 in *T. brucei* [43,44].

CAP5.5 was one protein identified uniquely in membrane preparations of virulent metacyclic, but not avirulent logarithmic promastigotes (see Table 2). A possible homologue was detected in the membrane skeleton of *Crithidia fasciculata* [44] but this is the first report of its presence in *Leishmania* spp. CAP5.5 in *T. brucei* is both myristoylated and palmitoylated, this type of doubly acylation is exclusively found in membrane associated proteins [45]. Furthermore, acylation has been found as a unique method for protein export in *Leishmania* spp. [46], indicating it may signal unique trafficking within the parasite cell. Similar to our findings in *L. chagasi*, CAP5.5 of *T. brucei* is stage specific, only expressed in procyclic form but not in the long slender and short stumpy blood forms of trypanosomes [45]. This protein might be a virulence factor and marker for metacyclic leishmania promastigotes.

Metacyclogenesis is a vital process in the life cycle of *Leishmania* spp. Metacyclic promastigotes are highly resistant to complement-mediated lysis, and are capable of evading killing by professional microbicidal macrophages in mammalian hosts. Metacyclogenesis is accompanied by a dramatic thickening of the parasite's cell coat. An approximately 10 nm thickening occurs during metacyclogenesis in *L. braziliensis* promastigotes, primarily due to a 2–3 fold increase in the size of the surface lipophosphoglycan [9–11]. There is incomplete information on the changes to the protein components of the plasma membrane that accompany metacyclogenesis.

Using a proteomic approach we identified several dozen *L. chagasi* proteins in the membranes of logarithmic growth phase and metacyclic promastigotes, most of which were stage-specific. Notably, several nutrient or proton transporters were uniquely present in the membrane fractions of avirulent logarithmic growth phase promastigotes. These included proton ATPase, pteridine transporter 3 and 6, vacuolar-type proton translocating pyrophosphatase 1 and zinc transporter-like protein. Furthermore, four heat shock proteins, two stress-induced proteins and several metabolic enzymes were also found exclusively in these cells. The latter included long-chain fatty acyl CoA synthetase, methionyl-tRNA synthetase, n-acyl-L-amino acid amidohydrolase, phosphoglyconate dehydrogenase, and probable citrate synthase. It is worth recalling that the metacyclic stage does not expend energy to undergo cell division, possibly explaining the presence of these proteins in membrane preparations from actively growing logarithmic cells. In contrast, well-characterized virulence factors including four MSP proteins and one GP46 were exclusively identified in the membranes of metacyclic promastigotes. Additionally, there were 24 and 10 putative proteins identified uniquely in logarithmic and metacyclic promastigotes, respectively. These deserve further investigation to determine their function and roles in pathogenesis as well as their usage as stage-specific markers.

We conclude from our proteomic approach that cellular fractionation and detergent extraction is an efficient means of obtaining enriched plasma membrane fractions. Plasma membrane proteins from logarithmically growing, metabolically active *L. chagasi* promastigotes contained stage-specific proteins required for nutrient acquisition or proton transport, as well as stress-related proteins and metabolic enzymes. In contrast, some well-characterized virulence factors were detected exclusively in plasma membrane preparations from metacyclic promastigotes. The largely non-overlapping lists of membrane proteins demonstrate the dramatic extent to which plasma membrane proteins undergo stage-specific modifications during developmental changes in the life cycle of the *Leishmania* spp. parasites.



## Supplementary Material

Refer to Web version on PubMed Central for supplementary material.

## Abbreviations

<b>βME</b>	β-mercaptoethanol
<b>GPI</b>	glycosylphosphatidylinositol
<b>HBSS</b>	Hanks' balanced salt solution
<b>MSP</b>	major surface proteases
<b>RT</b>	room temperature
<b>TMD</b>	transmembrane domain

## References

1. Bates PA. Transmission of *Leishmania* metacyclic promastigotes by phlebotomine sand flies. *Int. J. Parasitol* 2007;37:1097–1106. [PubMed: 17517415]
2. da Silva R, Sacks DL. Metacyclogenesis is a major determinant of *Leishmania* promastigote virulence and attenuation. *Infect. Immun* 1987;55:2802–2806. [PubMed: 3666964]
3. Sacks DL. Metacyclogenesis in *Leishmania* promastigotes. *Exp. Parasitol* 1989;69:100–103. [PubMed: 2659372]
4. Spath GF, Beverley SM. A lipophosphoglycan-independent method for isolation of infective *Leishmania* metacyclic promastigotes by density gradient centrifugation. *Exp. Parasitol* 2001;99:97–103. [PubMed: 11748963]
5. Svensjo E, Batista PR, Brodskyn CI, Silva R, et al. Interplay between parasite cysteine proteases and the host kinin system modulates microvascular leakage and macrophage infection by promastigotes of the *Leishmania donovani* complex. *Microbes Infect* 2006;8:206–220. [PubMed: 16203170]
6. Yao C, Chen Y, Sudan B, Donelson JE, Wilson ME. *Leishmania chagasi*: Homogenous metacyclic promastigotes isolated by buoyant density are highly virulent in a mouse model. *Exp. Parasitol* 2008;118:129–133. [PubMed: 17706646]
7. Garcia, LS. *Diagnostic Medical Parasitology*. Washington, DC: ASM Press; 2001.
8. Sacks, D.; Lawyer, P.; Kamhawi, S. *Leishmania After the Genome*. Myler, P.; Fasel, N., editors. Norfolk, UK: Caister Academic Press; 2008. p. 205-238.
9. McConville MJ, Turco SJ, Ferguson MA, Sacks DL. Developmental modification of lipophosphoglycan during the differentiation of *Leishmania major* promastigotes to an infectious stage. *EMBO J* 1992;11:3593–3600. [PubMed: 1396559]
10. Pinto-da-Silva LH, Camurate M, Costa KA, Oliveira SM, et al. *Leishmania (Viannia) braziliensis* metacyclic promastigotes purified using *Bauhinia purpurea* lectin are complement resistant and highly infective for macrophages *in vitro* and hamsters *in vivo*. *Int. J. Parasitol* 2002;32:1371–1377. [PubMed: 12350372]
11. Sacks DL, Pimenta PF, McConville MJ, Schneider P, Turco SJ. Stage-specific binding of *Leishmania donovani* to the sand fly vector midgut is regulated by conformational changes in the abundant surface lipophosphoglycan. *J. Exp. Med* 1995;181:685–697. [PubMed: 7836922]
12. Handman, E.; Papenfuss, AT.; Speed, TP.; Goding, JW. *Leishmania After the Genome*. Myler, P.; Fasel, N., editors. Norfolk, UK: Caister Academic Press; 2008. p. 177-204.
13. Yao C, Donelson JE, Wilson ME. The major surface protease (MSP or GP63) of *Leishmania* sp. Biosynthesis, regulation of expression, and function. *Mol. Biochem. Parasitol* 2003;132:1–16. [PubMed: 14563532]
14. Wilson ME, Hardin KK. The major concanavalin A-binding surface glycoprotein of *Leishmania donovani chagasi* promastigotes is involved in attachment to human macrophages. *J. Immunol* 1988;141:265–272. [PubMed: 3379307]

15. Yao C, Donelson JE, Wilson ME. Internal and surface-localized MSP of *Leishmania* and their differential release from promastigotes. *Eukaryot. Cell* 2007;6:1905–1912. [PubMed: 17693594]
16. Yao C, Luo J, Hsiao C, Donelson JE, Wilson ME. Internal and surface subpopulations of the major surface protease (MSP) of *Leishmania chagasi*. *Mol. Biochem. Parasitol* 2005;139:173–183. [PubMed: 15664652]
17. Yao C, Luo J, Storlie P, Donelson JE, Wilson ME. Multiple products of the *Leishmania chagasi* major surface protease (MSP or GP63) gene family. *Mol. Biochem. Parasitol* 2004;135:171–183. [PubMed: 15110459]
18. Russell DG, Wilhelm H. The involvement of the major surface glycoprotein (gp63) of *Leishmania* promastigotes in attachment to macrophages. *J. Immunol* 1986;136:2613–2620. [PubMed: 3950420]
19. Wilson ME, Hardin KK, Donelson JE. Expression of the major surface glycoprotein of *Leishmania donovani chagasi* in virulent and attenuated promastigotes. *J. Immunol* 1989;143:678–684. [PubMed: 2738406]
20. Liu X, Chang KP. Identification by extrachromosomal amplification and overexpression of a zeta-crystallin/NADPH-oxidoreductase homologue constitutively expressed in *Leishmania* spp. *Mol. Biochem. Parasitol* 1994;66:201–210. [PubMed: 7808470]
21. Berriman M, Ghedin E, Hertz-Fowler C, Blandin G, et al. The genome of the African trypanosome *Trypanosoma brucei*. *Science* 2005;309:416–422. [PubMed: 16020726]
22. El-Sayed NM, Myler PJ, Bartholomeu DC, Nilsson D, et al. The genome sequence of *Trypanosoma cruzi*, etiologic agent of Chagas disease. *Science* 2005;309:409–415. [PubMed: 16020725]
23. Ivens AC, Peacock CS, Worthey EA, Murphy L, et al. The genome of the kinetoplastid parasite, *Leishmania major*. *Science* 2005;309:436–442. [PubMed: 16020728]
24. Peacock CS, Seeger K, Harris D, Murphy L, et al. Comparative genomic analysis of three *Leishmania* species that cause diverse human disease. *Nat. Genet* 2007;39:839–847. [PubMed: 17572675]
25. Silverman JM, Chan SK, Robinson DP, Dwyer DM, et al. Proteomic analysis of the secretome of *Leishmania donovani*. *Genome Biol* 2008;9:R35. [PubMed: 18282296]
26. Pshezhetsky AV, Fedjaev M, Ashmarina L, Mazur A, et al. Subcellular proteomics of cell differentiation: Quantitative analysis of the plasma membrane proteome of Caco-2 cells. *Proteomics* 2007;7:2201–2215. [PubMed: 17549793]
27. Clifton JG, Li X, Reutter W, Hixson DC, Josic D. Comparative proteomics of rat liver and Morris hepatoma 7777 plasma membranes. *J. Chromatogr. B Analyt. Technol. Biomed. Life Sci* 2007;849:293–301.
28. Berro R, de la Fuente C, Klase Z, Kehn K, et al. Identifying the membrane proteome of HIV-1 latently infected cells. *J. Biol. Chem* 2007;282:8207–8218. [PubMed: 17237230]
29. Delvecchio VG, Connolly JP, Alefantis TG, Walz A, et al. Proteomic profiling and identification of immunodominant spore antigens of *Bacillus anthracis*, *Bacillus cereus*, and *Bacillus thuringiensis*. *Appl. Environ. Microbiol* 2006;72:6355–6363. [PubMed: 16957262]
30. Xie J, Techritz S, Haebel S, Horn A, et al. A two-dimensional electrophoretic map of human mitochondrial proteins from immortalized lymphoblastoid cell lines: a prerequisite to study mitochondrial disorders in patients. *Proteomics* 2005;5:2981–2999. [PubMed: 15986334]
31. Coonrod SA, Wright PW, Herr JC. Oolemmal proteomics. *J. Reprod. Immunol* 2002;53:55–65. [PubMed: 11730904]
32. Jang JH, Hanash S. Profiling of the cell surface proteome. *Proteomics* 2003;3:1947–1954. [PubMed: 14625857]
33. Sabarth N, Lamer S, Zimny-Arndt U, Jungblut PR, et al. Identification of surface proteins of *Helicobacter pylori* by selective biotinylation, affinity purification, and two-dimensional gel electrophoresis. *J. Biol. Chem* 2002;277:27896–27902. [PubMed: 12023975]
34. Shin BK, Wang H, Yim AM, Le Naour F, et al. Global profiling of the cell surface proteome of cancer cells uncovers an abundance of proteins with chaperone function. *J. Biol. Chem* 2003;278:7607–7616. [PubMed: 12493773]

35. Zhang W, Zhou G, Zhao Y, White MA. Affinity enrichment of plasma membrane for proteomics analysis. *Electrophoresis* 2003;24:2855–2863. [PubMed: 12929181]
36. Zhao Y, Zhang W, Kho Y. Proteomic analysis of integral plasma membrane proteins. *Anal. Chem* 2004;76:1817–1823. [PubMed: 15053638]
37. Bridges DJ, Pitt AR, Hanrahan O, Brennan K, et al. Characterisation of the plasma membrane subproteome of bloodstream form *Trypanosoma brucei*. *Proteomics* 2008;8:83–99. [PubMed: 18095354]
38. Lopez-Villar E, Monteoliva L, Larsen MR, Sachon E, et al. Genetic and proteomic evidences support the localization of yeast enolase in the cell surface. *Proteomics* 2006;(6 Suppl 1):S107–S118. [PubMed: 16544286]
39. Miles LA, Dahlberg CM, Plescia J, Felez J, et al. Role of cell-surface lysines in plasminogen binding to cells: identification of alpha-enolase as a candidate plasminogen receptor. *Biochemistry* 1991;30:1682–1691. [PubMed: 1847072]
40. Pancholi V. Multifunctional alpha-enolase: its role in diseases. *Cell. Mol. Life Sci* 2001;58:902–920. [PubMed: 11497239]
41. Pancholi V, Fischetti VA. alpha-enolase, a novel strong plasmin(ogen) binding protein on the surface of pathogenic streptococci. *J. Biol. Chem* 1998;273:14503–14515. [PubMed: 9603964]
42. Quinones W, Pena P, Domingo-Sananes M, Caceres A, et al. *Leishmania mexicana*: molecular cloning and characterization of enolase. *Exp. Parasitol* 2007;116:241–251. [PubMed: 17382932]
43. Hou WY, Pimenta PF, Shen RL, Da Silva PP. Stereo views and immunogold labeling of the pellicular microtubules at the inner surface of the plasma membrane of *Leishmania* as revealed by fracture-flip. *J. Histochem. Cytochem* 1992;40:1309–1318. [PubMed: 1506668]
44. Seebeck T, Kung V, Wylter T, Muller M. A 60-kDa cytoskeletal protein from *Trypanosoma brucei brucei* can interact with membranes and with microtubules. *Proc. Natl. Acad. Sci. USA* 1988;85:1101–1104. [PubMed: 3422481]
45. Hertz-Fowler C, Ersfeld K, Gull K. CAP5.5, a life-cycle-regulated, cytoskeleton-associated protein is a member of a novel family of calpain-related proteins in *Trypanosoma brucei*. *Mol. Biochem. Parasitol* 2001;116:25–34. [PubMed: 11463463]
46. Denny PW, Gokool S, Russell DG, Field MC, Smith DF. Acylation-dependent protein export in *Leishmania*. *J. Biol. Chem* 2000;275:11017–11025. [PubMed: 10753904]

## Acknowledgments

We are grateful to Dr. Donald L. Montgomery of the University of Wyoming for critical reviewing the manuscript and Dr. James D. Bangs of the University of Wisconsin for providing the rabbit polyclonal antibody to ER BiP protein. This work was supported by grants AI32135 and AI059451 (JED and MEW), and AI45540 and AI048822 (MEW) from the National Institutes of Health, two Merit Review grants (CY and MEW), an MERP (CY) and a Persian Gulf RFP (MEW) from the Department of Veterans' Affairs, and a start-up package from the University of Wyoming (CY).

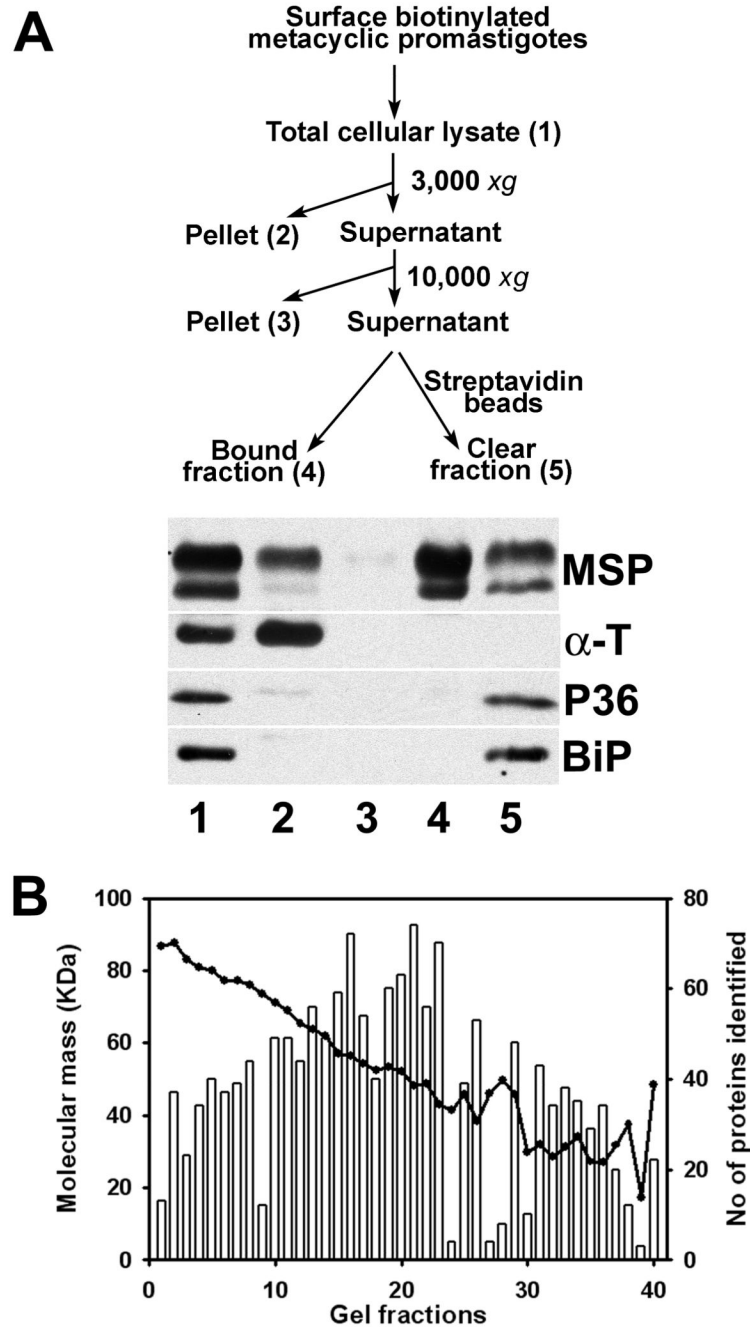


**Figure 1.** Identification of plasma membrane proteins by biotin-avidin affinity purification and LC-MS/MS. **A.** A flow chart of surface biotinylation and streptavidin isolation of plasma membrane proteins (top panel), and western blots showing the abundances of the major surface proteases (MSP) and cleanness of the preparation (lane 4) without detectable contaminants of cytoskeletal  $\alpha$ -tubulin ( $\alpha$ -T), cytosolic protein 36 (P36) and the luminal protein BiP of the endoplasmic reticulum. **B.** Numbers of protein identified (vertical bars) and the average molecular sizes in kDa (solid line) from each gel slice by LC-MS/MS. The 40 gel slices were generated from a silver-stained 5–15% gradient SDS-PAGE gel strip

loaded with the plasma-membrane proteins (Same as lane 4 in **A**) of  $2 \times 10^9$  cell equivalence.

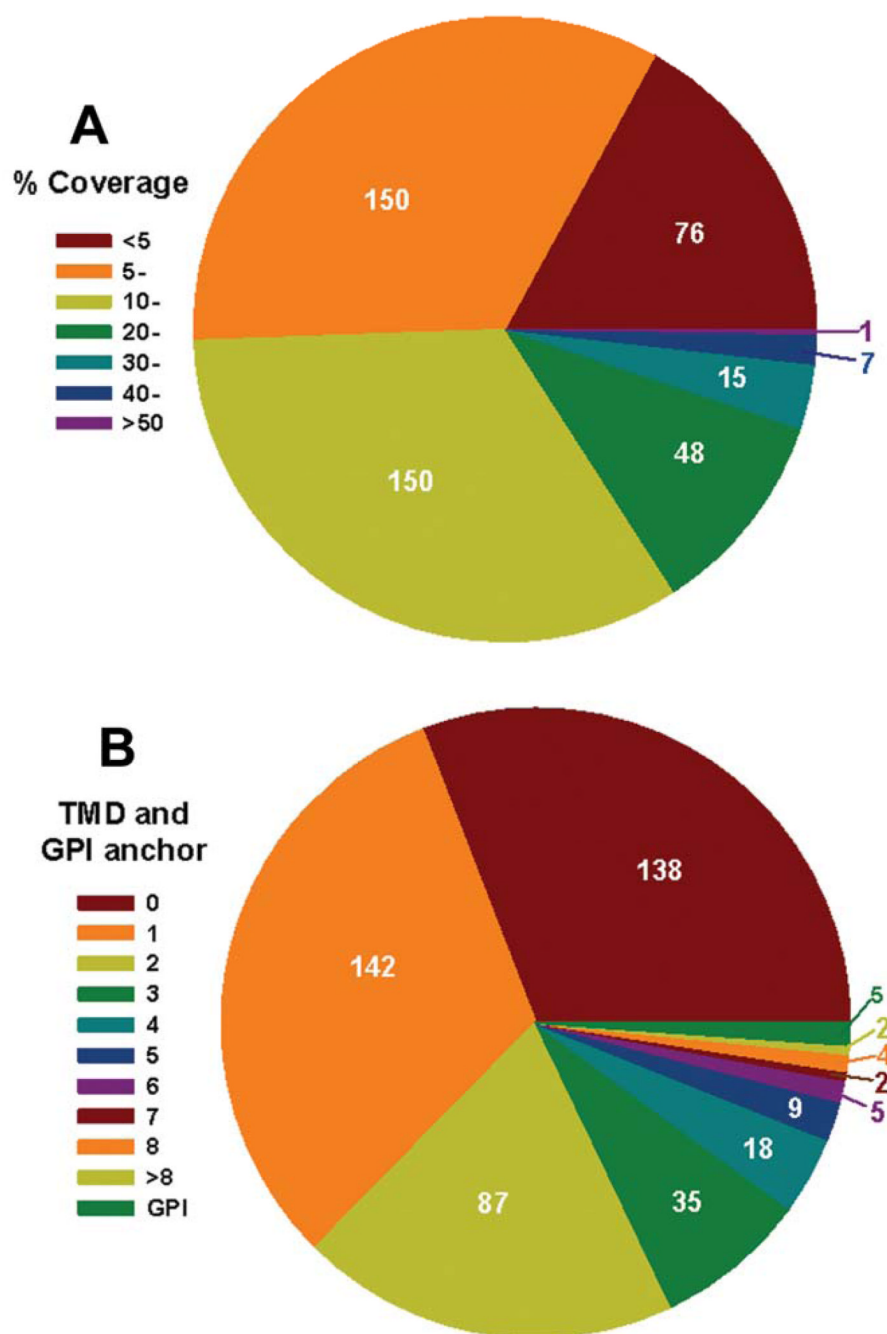


**Figure 2.** Percentage coverage (% amino acid) (**A**) and number of predicted transmembrane domains (TMD) and GPI anchors (**B**) of the 447 proteins detected using surface biotinylation-streptavidin affinity purification and LC-MS/MS.

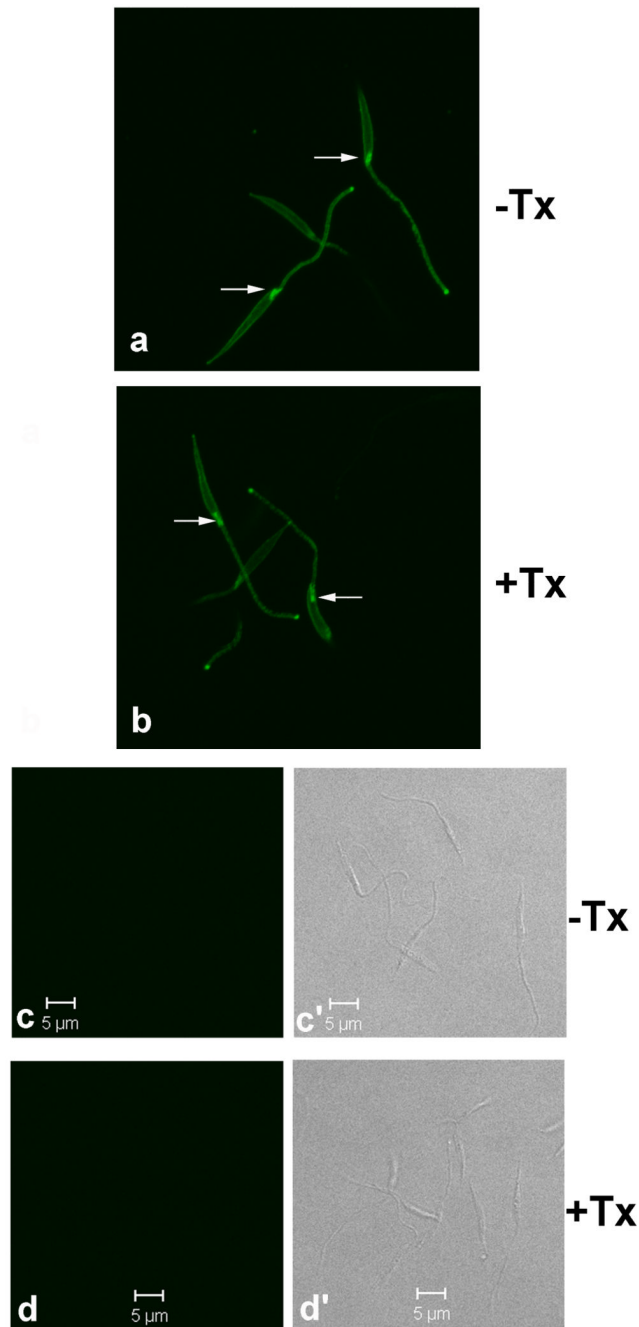


**Figure 3.**

Proteins in the flagellar pockets of metacyclic promastigotes are accessible to surface biotinylation. Metacyclic promastigotes were surface biotinylated in 1 mM Sulfo-NHS-biotin/HBSS (Panels a and b) or in HBSS alone (Panels c-c' and d-d'), followed by fixation in 10% PBS-buffered formalin. Afterwards, the cells were incubated in 0.2% Triton X-100 (+Tx)/PBS or in PBS alone (-Tx). Cells were then incubated in FITC-conjugated extravidin and observed by confocal microscopy at 0.3 μm for z-section. Panels a and b shown stacked z-sections generated by the open access ImageJ software ([rsbweb.nih.gov/ij/](http://rsbweb.nih.gov/ij/)). Biotinylated flagellar pockets are marked by arrows. No background staining is observed from non-biotinylated cells (c and d) with DIC (c' and d') to show the cells.

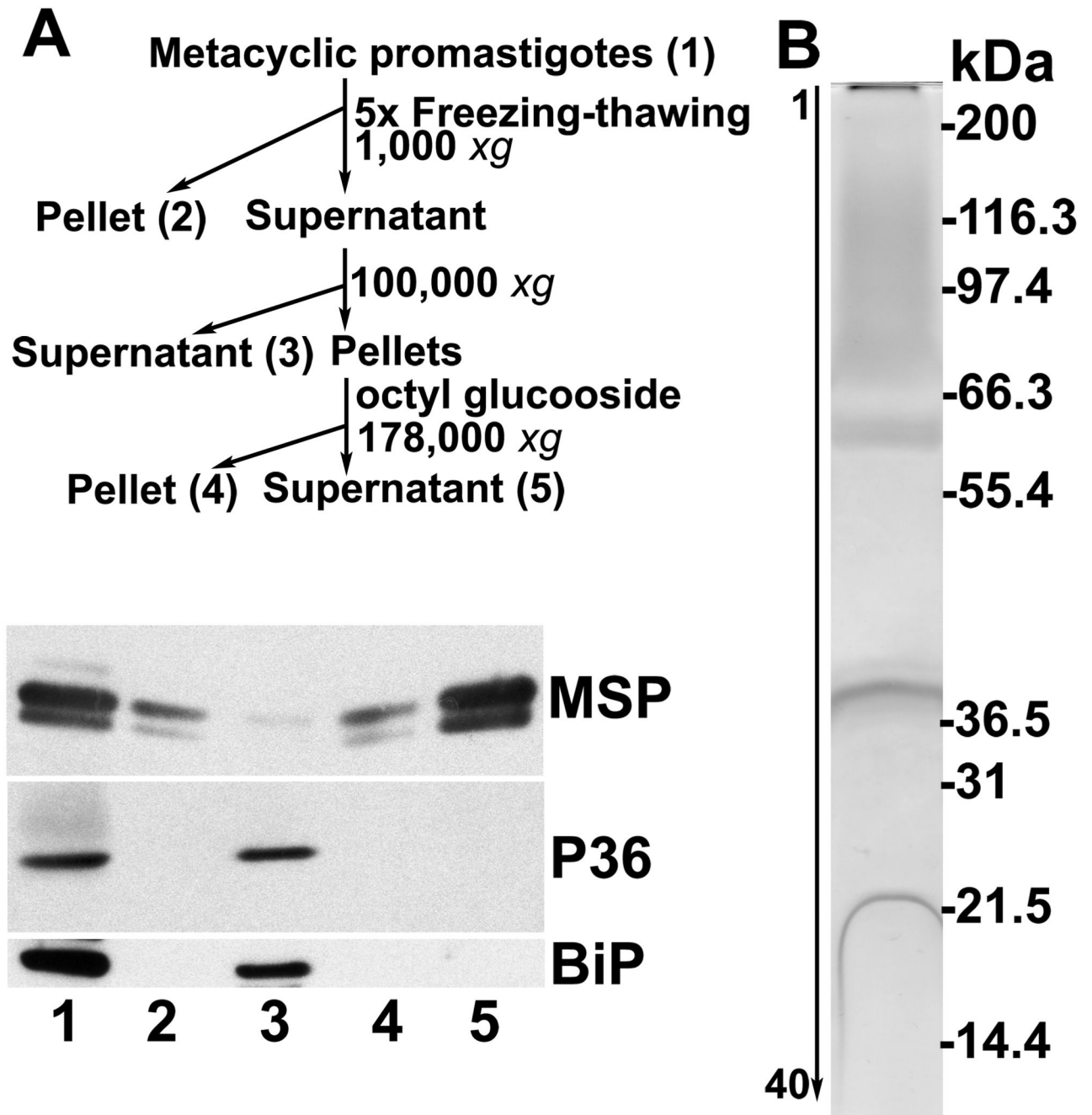


**Figure 4.**

**A.** Isolation of membrane proteins by detergent octyl glucoside extraction. Flow chart (top panel), and western blots showing abundance of MSP and cleanliness of the preparation (lane 5) without detectable contaminants of P36 and BiP. **B.** Silver-stained gel strip loaded with plasma-membrane proteins (same as lane 5 in **A**).  $2 \times 10^9$  cell equivalence was loaded onto a 5–15% gradient SDS-PAGE gel. Forty gel slices were excised from the lane and subjected to LC-MS/MS for protein identification. Locations of standard marker proteins in kDa are shown on the right.



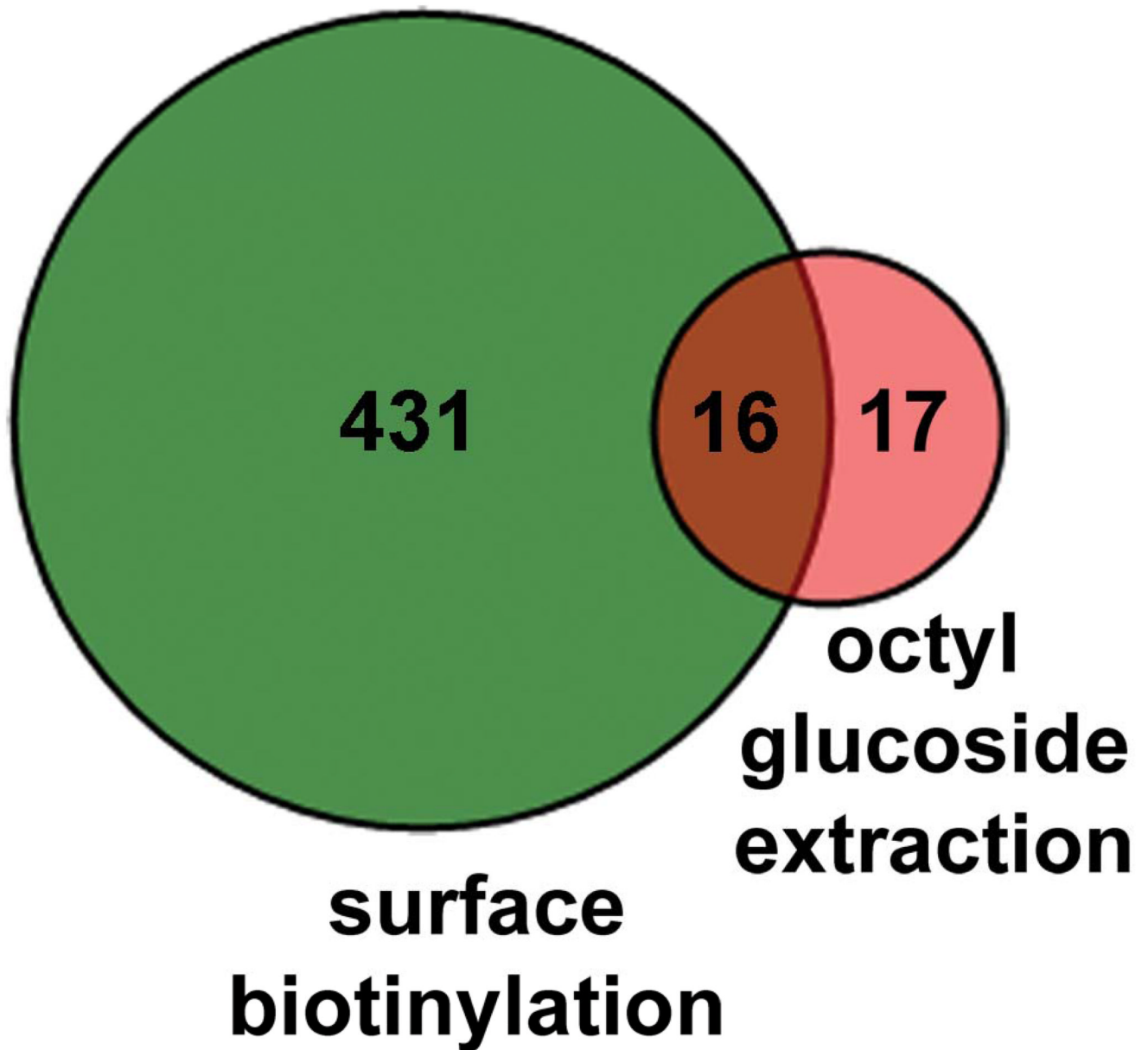


**Figure 5.**

Plasma membrane proteins detected by LC-MS/MS in the samples prepared by methods of biotin-avidin affinity purification and detergent extraction. A total of 447 and 33 proteins were identified, respectively. Of these, only 16 proteins were found in samples prepared by both methods.

**Table 1**

Common proteins identified by LC-MS/MS in the membrane fractions prepared by live cell biotinylation or octyl glucoside extraction.

FUNCTION	ACCESSION	Da	pI	TMD	%AA	Peptides found
Alpha tubulin	A4H727	53521.4	5.03	1	22.06	7
Beta tubulin	P21148	50020.8	4.57	2	24.49	8
CPC cysteine peptidase	A4I4D6	36995.8	5.10	3	20.00	5
Cytoskeleton-associated protein CAP5.5	A4I6E4	79917.3	5.39	1	11.33	7
Enolase	A4HW62	46008.1	5.20	1	41.19	12
Fructose-1,6-bisphosphate aldolase	A4ICK8	40694.6	8.68	1	18.60	6
MSP#	P23223	62911.0	6.42	4	5.76	2
MSP#	Q27673	63013.1	6.91	2	3.93	3
MSP#	A4HUF6	63517.4	6.96	5	15.05	6
MSP#	P15706	63808.6	6.83	4	37.40	21
MSP	A4I3D1	60546.0	7.41	4	15.34	6
Nucleoside diphosphate kinase	Q9GP00	16614.5	8.18	1	59.60	8
Proteasome alpha 1 subunit	A4HP20	29725.7	5.04	0	15.09	3
Proteasome alpha 7 subunit	A4H9T4	34861.8	7.39	0	14.61	3
Vacuolar ATP synthase catalytic subunit a	A4IAD4	67676.0	4.97	2	3.77	2
Vacuolar ATP synthase catalytic subunit a	A4HB86	67370.9	5.06	2	8.85	4

# Predicted to have a GPI anchor

Table 2

Differential expression of plasma membrane proteins in logarithmic (Log) versus metacyclic (Meta) promastigotes of *L. chagasi*.

FUNCTION	ACCESSION	Da	pI	TMD	Log (AA%)	Meta (AA%)	Peptides found
ADP-ATP carrier protein 1, mitochondrial precursor	A4H9X7	35545.00	10.05	5	4.98	9.35	2
Alpha tubulin	A4H727	53521.40	5.03	1	6.39	10.10	4
Beta tubulin	P21148	50020.80	4.57	2	7.19	6.53	3
Enolase	A4HW62	46008.10	5.20	1	7.46	3.77	2
Gim5A protein, putative; glycosomal membrane	A4HN41	24812.8	8.51	3	11.56	12.44	2
Histone H4	A4HSP4	11418.20	10.89	0	18.00	18.00	2
Kinesin	A4H0A6	75199.00	9.84	1	5.03	3.81	3
Kinetoplastid membrane protein 11B	Q25297	11170.40	6.25	0	46.74	27.17	5
Lanosterol 14-alpha-demethylase	A2TEF2	54119.70	7.62	3	6.46	6.46	2
MSP#	P15706	63808.60	6.83	4	5.34	6.84	4
Paraflagellar rod component	A4HU55	68098.33	5.09	1	4.79	7.60	4
Paraflagellar rod protein 1D	A4HIY0	69219.20	5.29	0	17.48	21.01	15
Paraflagellar rod protein 2C	A4HX39	68860.50	5.28	0	8.51	15.53	9
Paraflagellar rod protein 2C	A4H8S1	68544.30	5.35	0	8.85	9.02	5
Putative	A4H8W1	36235.20	5.87	1	8.83	6.94	2
Putative	A4HYD4	41395.10	4.88	1	9.70	9.43	3
Putative	A4HZY8	49801.80	5.49	0	22.78	5.69	8
Putative	A4H0B5	62548.10	6.59	3	14.21	8.45	7
Putative	A4H0F1	14558.30	4.07	0	24.43	24.43	2
Putative	A4HDT7	71114.90	5.63	1	7.52	5.76	5
Soluble n-ethylmaleimide sensitive factor	A4HYZ8	32034.60	4.99	0	14.89	9.57	4
Ubiquitin	Q05550	8544.60	7.58	0	32.89	44.74	2
Vacuolar ATPase subunit-	A4H4F9	41620.60	4.89	0	13.45	7.00	4

FUNCTION	ACCESSION	Da	pI	TMD	Log (AA%)	Meta (AA%)	Peptides found
like protein							
Vacuolar ATPase subunit-like protein	A4HSN6	41528.50	4.70	0	13.45	5.04	4
19S proteasome regulatory subunit	A4HBS3	54334.20	6.01	0	5.49		2
22 kDa potentially aggravating protein papLe22	Q9NJS2	22098.40	9.32	3	6.60		2
Acyl carrier protein	A4HFE7	16705.60	5.93	0	21.33		2
ATP-dependent RNA helicase	A4HMX7	94335.70	6.13	1	5.47		4
Calmodulin	Q25420	15481.50	4.09	0	24.29		2
Cytochrome b5-like	A4HSX6	13146.60	4.70	1	24.79		2
Cytochrome C oxidase subunit VI	A4HZH7	19241.30	7.96	0	19.75		2
DNAJ domain protein	A4I0P2	88800.40	5.93	4	4.16		2
Dynein arm light chain	A4I0S3	27254.10	5.63	0	10.13		2
Eukaryotic translation initiation factor	A4HGT5	46318.30	4.92	1	21.48		6
Gim5A protein	A4IBQ9	24783.70	8.63	3	12.44		2
Heat shock protein	Q4QDQ2	91746.30	5.02	1	3.52		2
Heat shock protein 83	P27890	52658.60	5.54	0	7.08		3
Heat shock protein 83-1	A4HL69	41393.60	4.80	0	6.96		2
Heat shock protein 83	P27741	80534.30	4.85	1	5.28		3
Long chain fatty Acyl CoA synthetase	A4HRT4	78855.60	7.63	3	3.84		2
Methionyl-tRNA synthetase	A4HZ82	84145.70	5.63	1	3.61		2
n-Acyl-L-amino acid amidohydrolase	A4HZ04	42737.60	5.02	2	7.34		2
Phosphogluconate dehydrogenase	Q18L02	51912.10	5.74	4	6.89		2
Poly(a)-binding protein	A4HDV5	62023.60	9.42	0	3.62		2
Probable citrate synthase	A4HXU4	52159.60	7.89	2	7.02		2
Probable proton ATPase 1A	P11718	107410.60	5.29	9	6.98		6

FUNCTION	ACCESSION	Da	pI	TMD	Log (AA%)	Meta (AA%)	Peptides found
Proteasome activator protein pa26	A4IAX3	23945.40	5.23	0	18.39		3
Proteasome alpha 7 subunit	A4H9T4	34861.80	7.39	0	7.14		2
Pteridine transporter ft3	A4HUE7	76188.40	6.10	14	4.43		2
Pteridine transporter ft6	A4HUE5	76005.20	5.63	14	1.88		2
Putative	A4H5E9	39862.50	6.41	0	7.02		3
Putative	A4H6H3	53945.60	8.43	4	6.22		3
Putative	A4H9P7	26979.60	7.33	0	10.64		2
Putative	A4HKK8	26364.00	5.46	0	11.64		2
Putative	A4HM53	14448.20	10.06	1	26.89		4
Putative	A4HQC5	84125.60	5.57	2	2.92		2
Putative	A4HTP3	42020.60	7.28	1	6.30		2
Putative	A4HTX5	93405.40	8.82	4	2.83		2
Putative	A4HWV0	36798.80	7.02	0	7.93		2
Putative	A4HXA8	36292.30	5.64	1	17.03		5
Putative	A4HZ55	11111.80	4.81	1	11.46		2
Putative	A4I0T3	13296.80	6.52	1	19.13		2
Putative	A4IIA0	11161.60	9.20	0	24.24		2
Putative	A4IIQ2	43111.40	6.44	3	9.14		2
Putative	A4I465	46343.40	5.84	2	15.88		5
Putative	A4I535	56359.60	4.82	0	36.48		12
Putative	A4I551	56465.10	8.08	0	5.34		2
Putative	A4I683	36279.50	6.32	5	7.78		2
Putative	A4I6L1	93786.00	8.92	6	2.38		2
Putative	A4I8B0	32807.20	4.92	1	11.00		2
Putative	A4IAY6	17953.00	7.24	0	16.97		2
Putative	A4IDM5	17414.60	8.55	0	24.38		3
Putative	A4IDN1	114046.50	7.16	7	2.18		2
Putative	A4IDT2	103400.70	6.83	4	3.01		2
Radial spoke protein 3	A4HFF8	42091.30	6.62	0	7.84		2

FUNCTION	ACCESSION	Da	pI	TMD	Log (AA%)	Meta (AA%)	Peptides found
Ribonucleoprotein p18, mitochondrial precursor	A4HWC9	21275.50	6.93	0	16.58		3
Ribonucleoprotein p18, mitochondrial precursor	A4HWD0	21305.50	6.93	0	8.56		2
Stress-induced protein sti1	A4H5F0	62414.10	6.11	0	6.22		3
Stress-induced protein sti1	A4HTP4	62201.10	5.84	0	5.13		2
Translation elongation factor 1-beta	A419P1	25920.50	5.00	0	12.13		2
Vacuolar-type proton translocating pyrophosphatase 1	A4HJA5	83592.20	4.86	16	5.36		3
Zinc transporter-like protein	A41745	48193.60	5.92	7	5.10		2
Adenylate nucleotide translocase	A7LBL5	36215.2	9.82	5		5.52	2
Calpain-like cysteine peptidase	A4HYX4	14987.30	5.18	0		16.03	2
CPC cysteine peptidase	A41D6	36995.8	5.10	3		20.00	5
Cysteine protease	Q8WT30	37009.8	5.10	3		15.88	4
Cytochrome C oxidase subunit VI	A4HD57	22258.30	6.24	0		14.80	2
Cytoskeleton-associated protein CAP5.5	A416E4	79917.3	5.39	1		7.87	4
Dehydrogenase-like protein	A4HUB6	44901.5	8.38	3		6.55	2
Enolase	A4H7T5	53692.20	7.89	3		6.81	2
Flagellar glycoprotein-like protein	A4HUH5	62330.0	7.66	5		6.24	3
Fructose-1,6-bisphosphate aldolase	A4ICK8	40694.6	8.68	1		7.01	2
Glycosomal membrane protein	A4I3V7	23759.8	10.25	2		13.96	2
Membrane-bound acid phosphatase precursor	A4ICG3	57288.5	7.67	3		5.45	3
MSP#	A4HUF6	63517.4	6.96	5		7.02	3
MSP#	P23223	62911.0	6.42	4		4.24	2
MSP#	Q27673	63013.1	6.91	2		2.51	2

FUNCTION	ACCESSION	Da	pI	TMD	Log (AA%)	Meta (AA%)	Peptides found
MSP	A4I3D1	60546.0	7.41	4		15.34	5
Paraflagellar rod protein ID	A4I4N5	69017.00	5.17	0		5.71	4
Proteasome alpha 1 subunit	A4HP20	29725.7	5.04	0		10.57	2
Proteasome alpha 7 subunit	A4H9T4	34861.8	7.39	0		7.14	2
Putative	A4H5E1	63469.70	4.58	2		3.51	2
Putative	A4HRM8	72826.10	5.40	2		3.33	2
Putative	A4HUH4	81190.5	5.94	9		2.91	2
Putative	A4I077	14107.10	7.84	0		17.80	2
Putative	A4I0D6	57285.50	7.76	3		5.88	2
Putative	A4I4S8	155409.8	5.24	10		3.48	4
Putative	A4I6U4	31523.70	8.19	0		9.93	2
Putative	A4I7J1	140540.3	5.01	6		4.22	5
Putative	A4I9W1	37830.4	7.75	3		15.34	4
Putative	A4IBR6	71206.1	6.39	5		3.84	2
Reiske iron-sulfur protein precursor	A4HMH5	33752.8	6.15	2		8.42	2
Reticulon domain protein	Q4Q737	22145.70	9.79	3		14.21	2
Surface Antigen Protein <sub>2</sub> #	A4HV45	43941.8	5.31	3		5.04	2
Vacuolar ATP synthase catalytic subunit a	A4HB86	67370.9	5.06	2		3.93	2
Vacuolar ATP synthase catalytic subunit a	A4IAD4	67676.0	4.97	2		3.77	2
Vacuolar proton translocating ATPase subunit A	A4I0M2	87674.00	4.92	7		4.26	2
Vesicle-associated membrane protein	A4H570	24223.40	8.24	1		11.63	2

# Predicted to have a GPI anchor